Journal of Applied Polymer Science

Study on Fracture Behavior of PLLA Transcrystallization: Effect of Crystalline Morphology

Tao Wen,[1] Xiuqin Zhang,[2] Zujiang Xiong,[1] Sicco de Vos,[3] Ruyin Wang,[4] Fosong Wang,[1] Dujin Wang[1]

[1]Beijing National Laboratory for Molecular Sciences, CAS Key Laboratory of Engineering Plastics, Institute of Chemistry, Chinese Academy of Sciences, Beijing 100190, China

[2]Beijing Key Laboratory of Clothing Materials R & D and Assessment, School of Materials Science & Engineering, Beijing Institute of Fashion Technology, Beijing 100029, China

[3]Purac Biochem B.V., Arkelsedijk 46, P.O. Box 21, 4200 AA Gorinchem, the Netherlands

[4]Purac China, Building 3, Yuanshan Road #318, Minhang District, Shanghai 201108, China

Correspondence to: D. Wang (E-mail: djwang@iccas.ac.cn)

ABSTRACT: In the present work, the fracture behavior of transcrystallization (TC) of poly(L-lactic acid) (PLLA) in thin film and the dependence of mechanical properties on the morphology of TC have been studied. The nucleation density of TC was merely determined by the annealing temperatures of the fibers which used for inducing nucleation, and the crystallization temperature and time of the samples were completely identical. By using *in situ* polarized optical microscopy, the fracture process of TCs was characterized. For the TC with high nucleating density (TC-H), lots of cracks were generated from the TC bulk during fracture. But only few cracks were observed on the TC with low nucleation density (TC-L), and the final fracture of TC-L always occurred in the junctions of crystal segments. Compared to the samples which do not contain TC, the fracture strength was enhanced by 8.1% because of the presence of TC-H. On the contrary, the presence of TC-L can reduce the fracture strength of the samples. The fracture surfaces of TC were characterized by scanning electron microscope. It was observed that the fracture surface of TC-H exhibited obvious fibrillation and cavitation, but the fracture surface of TC-L was smooth and featureless. The possible fracture mechanism for two TCs was discussed in view of their intrinsic crystal organizations. © 2014 Wiley Periodicals, Inc. J. Appl. Polym. Sci. **2015**, *132*, 41273.

KEYWORDS: crystallization; mechanical properties; morphology; polyesters; structure-property relations

Received 17 April 2014; accepted 5 July 2014

DOI: 10.1002/app.41273

INTRODUCTION

Transcrystallization (TC) is a well-known phenomenon which is usually observed in polymer composites.[1] The formation of TC is resulted from the high nucleating capability of polymer on the heterogeneous substrate, e.g., the surface of fiber or inorganic filler. Such solid surface can lead to an extremely high nucleation density, and then the lamellae were only allowed to develop along the direction perpendicular to the substrate, because of the space confinement.

Since TCs always form at the interface of polymers and fillers in the composites, it is believed that the formation and morphology of TCs are vital for the mechanical properties of materials. Many studies had focused on the influences of TCs on the performance of composites; however, the corresponding results reported by previous literatures were conflicting to each other. In some cases, it was found that the formation of TC improved the mechanical properties[2–9]; however, other cases showed that the TC did not affect the strength of composites,[10–12] or exhibited a negative effect.[13–16] Actually, there are several factors influencing the final experimental results, e.g., the testing methods, the natural properties of polymer and filler, and the preparation methods of samples. One of the problems is that, in order to prepare TCs with distinct morphologies, the preparation

The copyright line for this article was changed on 06 April 2015 after original online publication.

Additional Supporting Information may be found in the online version of this article.

Table I. Basic Information of Materials

	Mn[a] (kg/mol)	Mw[a] (kg/mol)	PDI	MFR[b] (g/10 min)	T_g (°C)	T_m (°C)
PLLA	152	226	1.49	6.9	57.5	175.4
PDLA	108	167	1.56	18.8	56.9	173.7

[a] Measured by SEC using chloroform as the eluent, low-angle laser light scattering (LALLS) detection and calibration against PS standards.
[b] Melt flow rate, 2.16 kg, 200°C.

conditions used for different samples were also different. For instance, a well-developed TC could be produced via slowly cooling from the melt with external inducements (e.g., fiber or plate), and the immature TC or fine spherulite could be prepared by quenching. Obviously, it is not reasonable to compare these two samples, because the differences between the samples were not only in the morphology, but also in other factors.

In our previous work, we found that the nucleation capability of poly(L-lactic acid)/poly(D-lactic acid) (PLLA/PDLA) blend fiber on PLLA matrix was determined by the crystalline type of the fiber.[17] Based on this observation, we found a new methodology that allowed us to prepare the TCs with different morphologies under same condition. Since the preparation conditions were completely identical, the mechanical properties of TCs exclusively depend on their morphologies. It helps us to gain a better understanding on the influence of TCs in the composites. Furthermore, in the present work, PLLA sample was reinforced by PLLA/PDLA blend fiber. The corresponding results may also provide detailed information for fabricating homogeneous fiber-reinforced PLLA composite with high performance.

EXPERIENTAL

Materials and Preparation of Blend

Samples of PLLA and PDLA were provided as pellets by Purac Biochem (Gorinchem, Netherlands), and both were used without further purification. The basic information of these materials was shown in Table I.

PLLA and PDLA pellets were dried at 80°C in a vacuum oven overnight before melt blending. The blend of PLLA and PDLA (50 : 50, wt %) was prepared using an internal mixer (Polylab OS, Thermo Scientific HAAKE) operated at 200°C with a rotation speed of 50 rpm for 5 min.

Preparation of Fibers and Transcrystallization

The preparation of PLLA/PDLA blend fibers and fiber-induced PLLA transcrystallization were discussed in our previous report.[17] Briefly, the blend fiber used in the present work was prepared by melt-spinning from a capillary rheometer (RH7, Bohlin). The as-spun fibers were annealed under drawing either at 145°C or 200°C for 60 min, respectively. The XRD results indicate that the blend fiber annealed at 145°C (named as BF145) mainly contained α-form crystal and the blend fiber annealed at 200°C (named as BF200) only contained stereocomplex (SC).[17]

The film of PLLA was prepared by compression-molding the polymer pellets at 190°C, and the thickness was about 30 μm. A piece of PLLA film with size of 5 mm × 25 mm was heated to 200°C for 3min on the glass slide covered by polyimide film. Firstly, the film was quenched to 175°C, and then the fiber which pre-fixed in a glass slide was carefully introduced onto the PLLA film. This placement was carefully controlled in order to ensure the fiber was located in the center of PLLA film and parallel to the edge of film. Subsequently, the sample was fast cooled to 130°C and isothermally crystallized for 15 min. Under the nucleating drive force, TC developed from fiber surface. Finally, the sample was cooled to room temperature and the glass slide was removed from the top of sample, and PLLA sample which containing TC and fiber was detached from substrate.

In Situ Polarized Optical Microscope Observation

In order to investigate the fracture behaviors of TCs, the stretching of sample was performed with Linkam tensile stage (TST 350). Before stretching, a notch was cut by blade in the edge of specimen for controlling the position where the fracture would take place (see Figure 1), and the size of notch was measured by optical microscopy. Then, PLLA specimen was fixed with the clamps, and the moving rate of clamps was 5 μm/s. With the increasing of clamp displacement, the crack initiated from the tip of notch and developed along the direction perpendicular to the fiber and TC. The mechanical curve of specimen was recorded by the tensile stage synchronously. The fracture process of TC was *in situ* observed by using an optical microscope (Olympus BX51) under polarized light and successively recorded by a camera. The quarter wavelength retardation plate was inset into the light path.

In the present work, the strength of the specimen was defined as the ratio of maximum stress (N) and the actual width of specimen (mm). The maximum stress was obtained from the peak value of curve. All the results were an average from at least 12 specimens.

Scanning Electron Microscopy

The morphology of fracture surface of PLLA TC was examined by using Scanning Electron Microscopy (SEM) (JSM-6700, JEOL) operated at 5 kV. The sample was coated with palladium layer (thickness: 5 nm) to avoid charging and thereby improving image quality.

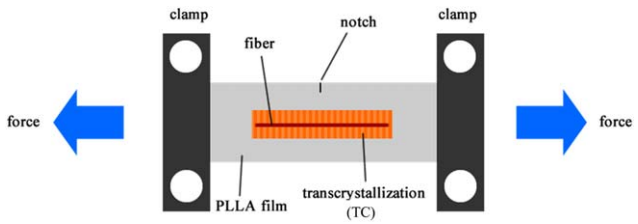

Figure 1. Mechanical sketch of tensile experiment on the PLLA specimen with fiber and TC. [Color figure can be viewed in the online issue, which is available at wileyonlinelibrary.com.]

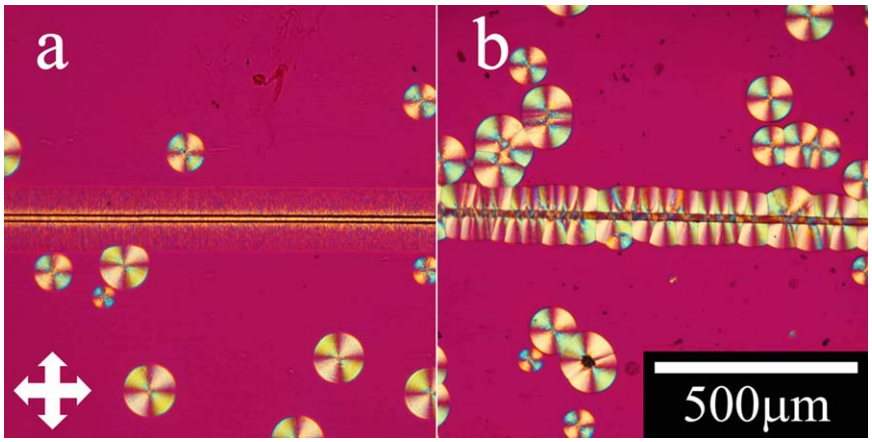

Figure 2. POM images of PLLA TCs induced by (a) BF145 and (b) BF200. The arrows indicated the crossed polarizers. [Color figure can be viewed in the online issue, which is available at wileyonlinelibrary.com.]

RESULTS AND DISCUSSION

Fracture of PLLA TC with Different Nucleation Densities

Figure 2 shows the polarized optical microscope (POM) images of PLLA TCs induced by different fibers. Because of the high nucleating capability of BF145, PLLA TC shown in Figure 2(a) exhibited extremely high nucleation density (named as TC-H). On the contrary, the nucleation density of TC induced by BF200 was much lower (named as TC-L). It is because that there is no epitaxial relationship between PLLA α form and SC.[17] The nucleation density of TC-L was ca. 0.03 μm^{-1}, and that of TC-H was too high to distinguish single nucleation. It is noteworthy that the neat PLLA fiber, which could also provide α crystal, was not used here, because of that the diameters of PLLA fiber and blend fiber were different after annealing.[17] It will be inconvenient for us to study the mechanical properties. However, the diameters of BF145 and BF200 were completely same after annealing.

As introduced before, the fracture behaviors of TCs with different nucleation densities were investigated. Since the difference between two TCs is merely the nucleation density and the crystallization temperature and time are totally identical, it is

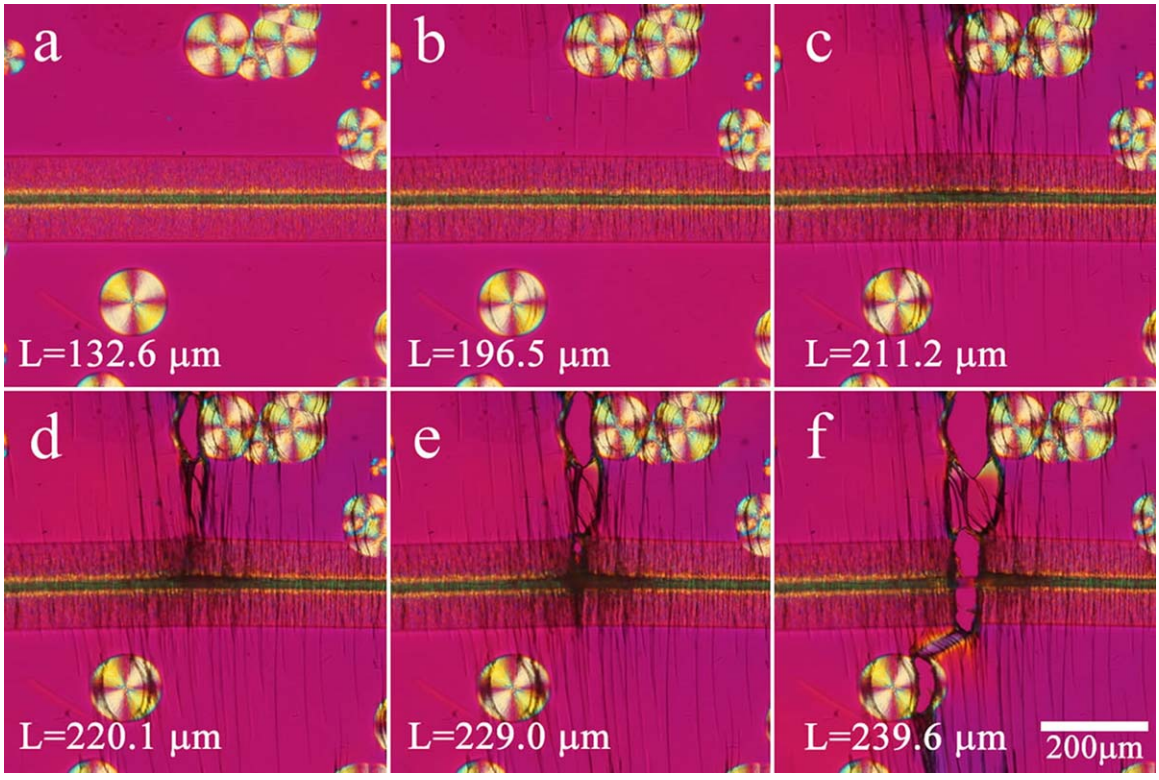

Figure 3. POM images of TC-H during fracture."L" indicated the clamp displacement value. [Color figure can be viewed in the online issue, which is available at wileyonlinelibrary.com.]

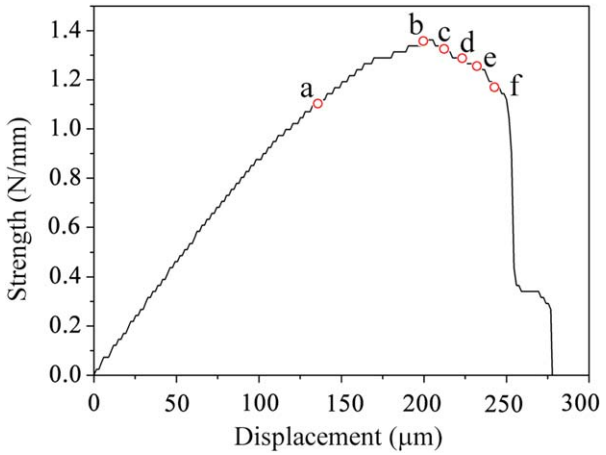

Figure 4. The typical strength–displacement curve of PLLA sample containing TC-H. "a"-"f" was related to the corresponding POM images in Figure 3. [Color figure can be viewed in the online issue, which is available at wileyonlinelibrary.com.]

reasonable to expect that the local crystallinity of two TCs should be same, i.e., the growth of crystal merely depends on the crystallization temperature and time. Thus, the mechanical properties of TCs exclusively depend on the morphologies, i.e., the nucleation densities. Firstly, we investigated the fracture behavior of TC-H. The continuous fracture process could be clearly observed via the video (Supporting Information, Video S1_TC-H. Note that the play speed of the video is three times faster than the actual situation). In Figure 3, the POM images of TC-H at different clamp displacements (L) were shown. The corresponding strength–displacement curve was shown in Figure 4, and the "a"–"f" marked on the curve related to the related images in Figure 3.

In Figure 4, it was found that the stress was fast increased with the displacement in initial stage. Meanwhile, before the main crack reached TC, lots of micro cracks were generated in the bulk of TC-H [Figure 3(a,b)]. It was observed that the most of the cracks were initiated at the interface of fiber and substrate. A reasonable interpretation is that the stress concentrated at the interface, thus leading to the generation of crack.[18] The max strength was reached before the main crack arrived in the TC, after then, the strength value gradually dropped off until the TC was completely fractured [Figure 3(f)]. During this process, the amount of the cracks remarkably raised with displacement. In the fracture region of TC-H, the density of crack was extremely high, which led to the local darkness in the POM image [Figure 3(d,e)]. Also, it should be pointed that the fiber did not break as soon as the crack completely passed through the TC. That is because the fiber was partly embedded in the substrate, and the detachment of fiber took place during stretching. The obvious failure of the specimen was occurred at the L of 250 μm, and the sample completely ruptured when L reached to 275 μm.

With the same method, the fracture behavior of TC-L was investigated (see Supporting Information, Video S2_TC-L). The POM images captured during the fracture process were shown in Figure 5, and the corresponding strength–displacement curve was shown in Figure 6. Some cracks could also be observed in

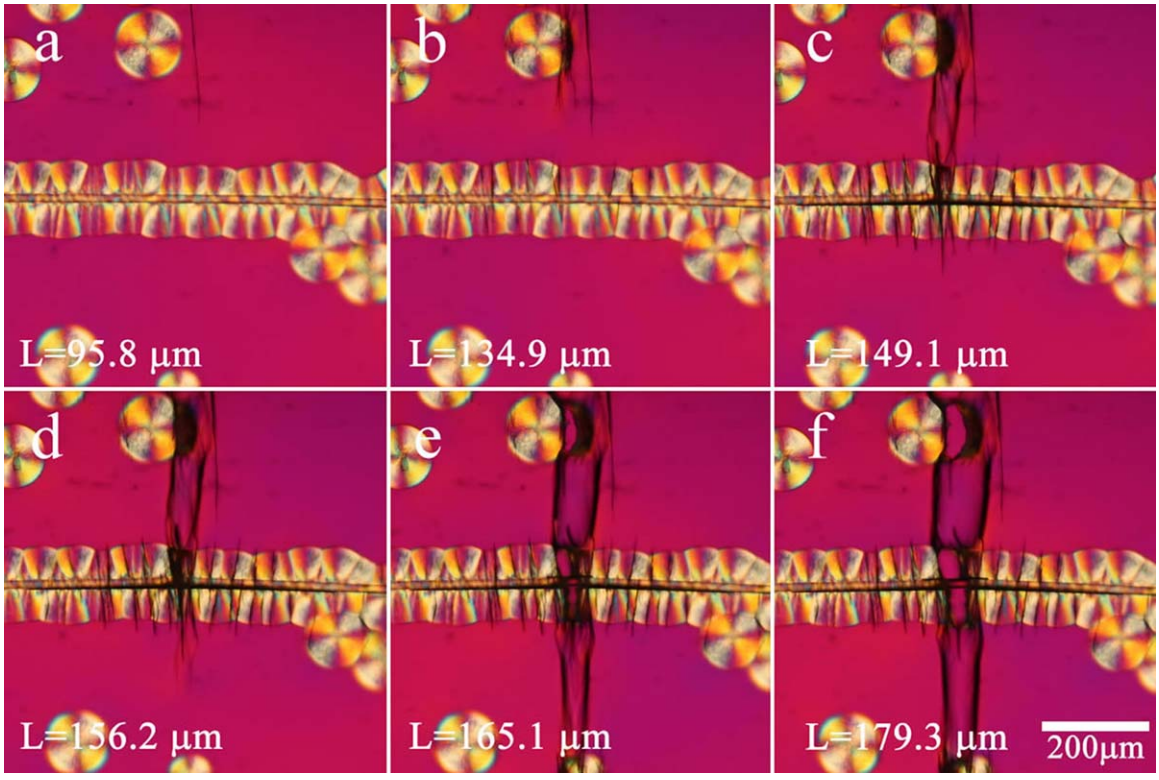

Figure 5. POM images of TC-L during fracture."L" indicated the clamp displacement value. [Color figure can be viewed in the online issue, which is available at wileyonlinelibrary.com.]

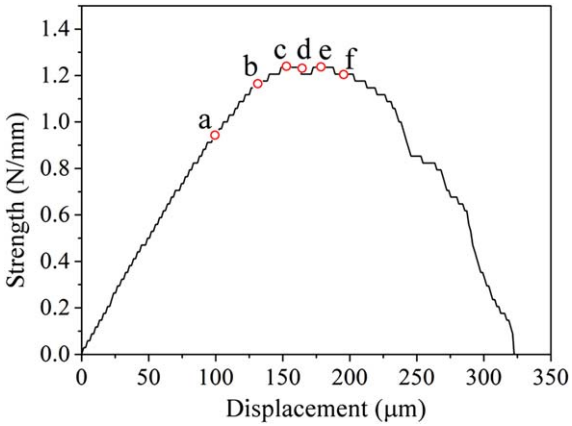

Figure 6. The typical strength–displacement curve of PLLA sample containing TC-L. "a"-"f" related to the corresponding POM images in Figure 5. [Color figure can be viewed in the online issue, which is available at wileyonlinelibrary.com.]

TC-L during stretching, but the number density was much lower compared with the result shown in Figure 3. In addition, it is noteworthy that the final failure of TC-L preferred to take place in the junction of adjacent crystal segments. It could be ascribed to the different organization of TCs with different nucleation densities. For TC-H, the nucleation density was extremely high and the lamellae were compactly stacked along the fiber. The entity of TC-H was closed to a rigid solid, so the crack easily generated in TC-H under external force. For TC-L, the nucleation density along the fiber was low, and there was adequate space between the nucleating points. Thus the crystal which initiated from individual nuclei site was allowed to grow independently, until it encountered the adjacent ones. In other words, the TC-L was constituted by many incomplete spherulite, thus the integral rigidity of TC-L was lower than that of TC-H. This will be discussed in detail later.

Table II. Strength of the Control Sample and the Samples with Different TCs

Sample	Strength (N/mm)	Variation
Control	1.35±0.13	—
TC-L	1.23±0.13	−8.9%
TC-H	1.52±0.14	12.6%

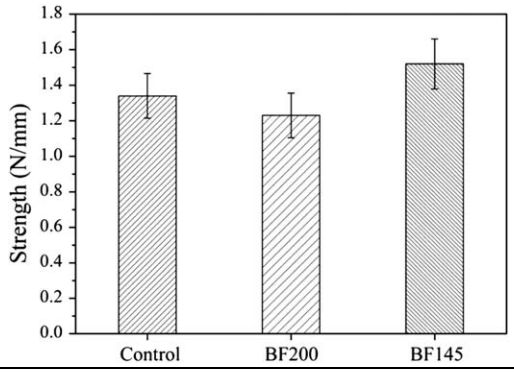

Table III. Strength of the Control Sample and the Samples with Different TCs

Sample	Strength (N/mm)	Variation
Control	1.35±0.13	-
TC-L	1.25 ±0.11	−7.4%
TC-H	1.46 ±0.12	8.1%

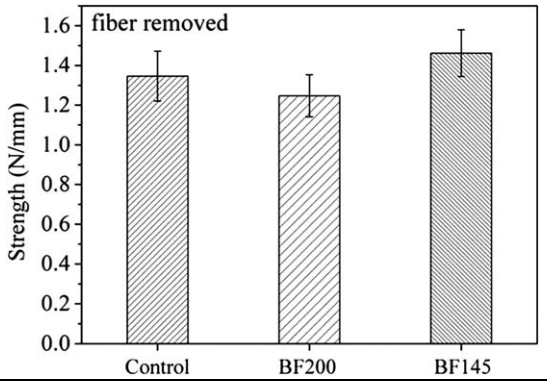

Mechanical Properties of TC

The fracture behaviors of TC with different morphologies were observed above. The crack was developed perpendicular to TC layer, so this result was related to the tear resistance of TC. For investigating the influence of TC on the mechanical properties, we prepared specimen through the same condition as above, but without any fiber (control sample), and the same tensile testing was performed. The result was compared with that of the samples containing fibers and TCs (Table II). It revealed that the strength of the sample with TC-H (1.52 ± 0.14 N/mm) was higher than that of control sample (1.35 ± 0.13 N/mm), which means the presence of TC-H improve the strength of PLLA sample. However, the strength of the sample containing TC-L was slightly decreased compared with the control sample.

The results shown in Table II were influenced by two factors: the morphology of TC and the interaction between fiber and substrate. Although the diameters of BF145 and BF200 were same, but the adhesion strengths between fibers and PLLA matrix were different, i.e., the adhesion strength between BF145 and PLLA substrate should be stronger than that between BF200 and PLLA. Because that α-form crystal in BF145 owns perfect lattice matching with PLLA matrix (homogeneous epitaxy), and there is no epitaxial relationship between SC crystal in BF200 and PLLA matrix.[17] It's well known that epitaxial crystallization can enhance the interfacial adhesion.[19–21] In order to exclude the impact of interfacial adhesion, the fibers were removed from the samples before tensile testing, and the results were only determined by TCs. By using POM and SEM, it was confirmed that removing the fibers did not make any damage to the samples. The fracture characteristics of TCs were still the same as that shown above (see Supporting Information, Figure S1). By comparing the results in Tables II and III, it was found that the influence on mechanical properties was mainly contributed by TC, rather than the adhesion between fiber and substrate. A possible reason is that the fiber was partially embedded

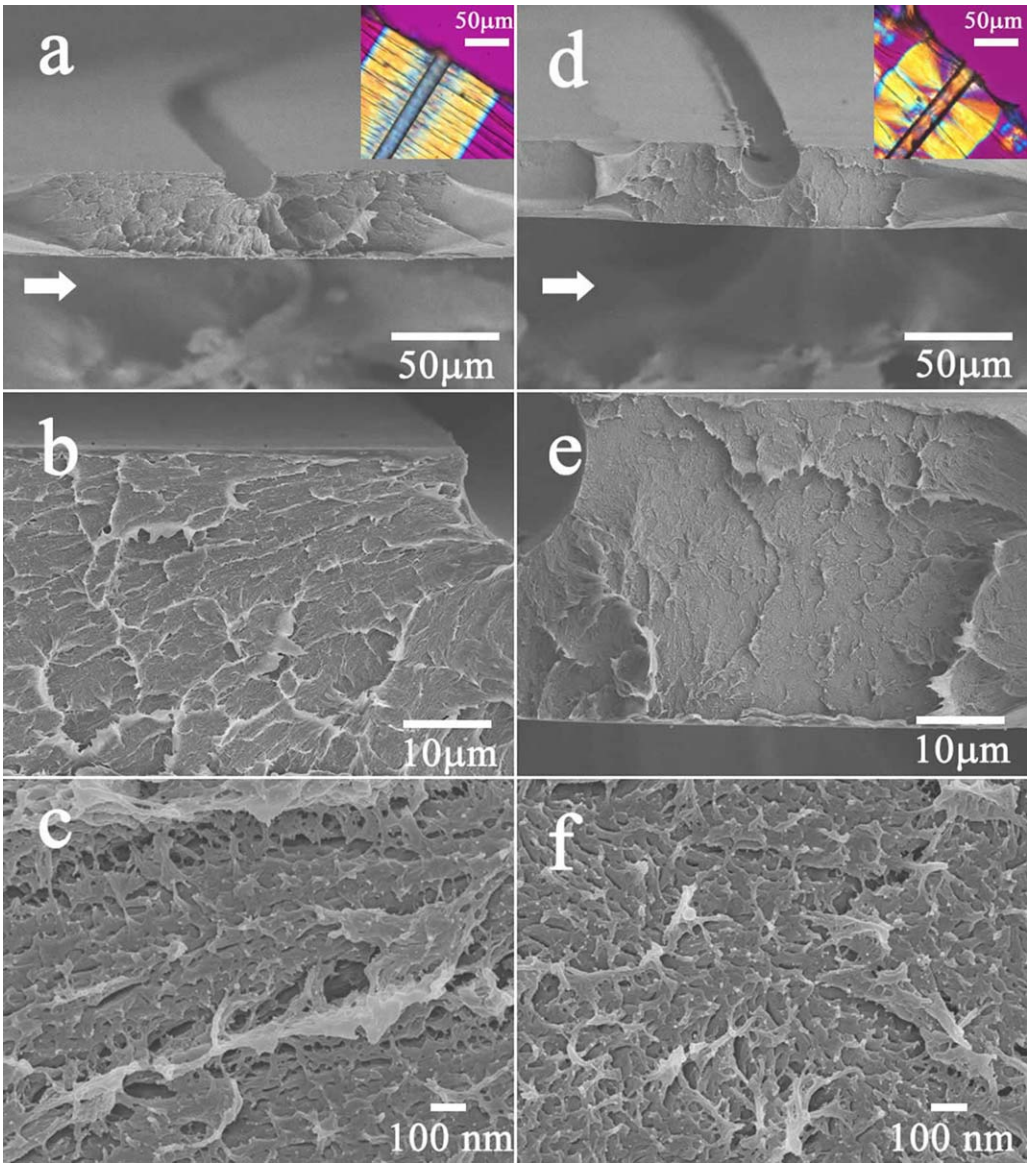

Figure 7. SEM images of fracture sections of (a–c) TC-H and (d–f) TC-L. Insets are the corresponding POM images. Arrows indicated the fracture directions. [Color figure can be viewed in the online issue, which is available at wileyonlinelibrary.com.]

by PLLA film, so that the interfacial bonding was minor because of the limited contact area.

Moreover, one may say the difference between the control samples and samples containing TCs shown in Tables II and III were not very remarkable. In fact, considering the content of TC in the sample, the variation of strength was apparent. The initial width of specimen was 5 mm and the width of notch was ca. 1 mm (Figure 1), so the actual width was ca. 4 mm. The width of TC was ca. 170 μm. The above result indicated that the strength was increased by 8.1%, while the TC-H merely accounts for only 4.5% of the whole specimen. That means the mechanical properties of PLLA sample was effectively improved by introducing a small fraction of TC-H. The amplification could even be higher (12.6%) before removing the fiber. On the contrary, the presence of TC-L reduced the strength of PLLA sample, which indicated that TC with low nucleation density led to a negative impact on the mechanical property. This will be discussed in detail later. Furthermore, it could be estimated that the strength of TC-H was 2.9 times of that of control sample (see Supporting Information).

SEM Observation on Fracture Surface

Above results indicated that the mechanical properties of TC strongly depended on their morphologies. In order to gain a better understanding, we investigated the morphology of the fracture surfaces of two TCs. Figure 7 shows the morphologies of the fracture surface of TC-H and TC-L. It was observed that a highly fibrillated damage zone was formed in the fracture surface of TC-H [Figure 7(b)]. The fibrils were radially distributed on the fracture surface around the location of fiber. The obvious fibrillation and cavitation indicated that the intense plastic deformation was occurred during the fracture process of TC-H. However, the fracture surface of TC-L was smooth and

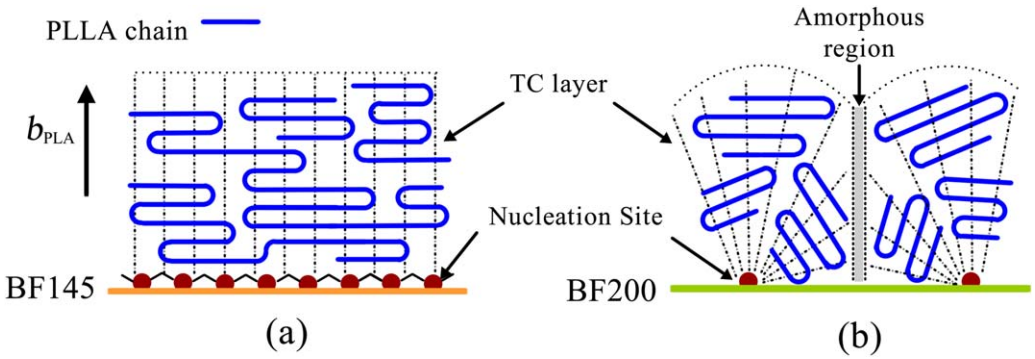

Figure 8. Illumination of crystalline structure of (a) TC-H and (b) TC-L. [Color figure can be viewed in the online issue, which is available at wileyonlinelibrary.com.]

featureless [Figure 7(e)]. Above results indicated that the extent of plastic deformation was much lower in TC-L, compared to TC-H.

It was known that the plastic deformation was resulted from the damage of crystals.[22] So the tearing belt shown in Figure 7(b) exhibited radial orientation [Figure 7(b)], because the lamellae were radially oriented in TC-H. However, the fracture surface of TC-L implied that less crystal frame was involved. Above results could be ascribed to the different integral structures of TCs (Figure 8). For TC-H, the nuclei sites were close to each other and the crystallization initiated from different nuclei and developed along the same direction simultaneously, i.e., perpendicular to fiber, because of the space confinement. Thus, the tight connections were allowed to construct between the adjacent lamellae via branching or tie molecules [Figure 8(a)]. Such connection resulted in a strong transverse strength of TC-H. The fracture of TC-H gave rise to the intense fibrillation and cavitation because of the deformation and damage of crystal organization. For TC-L, the crystal which initiated from an individual nucleus was developing outward without spacial restraint until it encountering the other one. In other word, the TC-L was constituted by many isolated crystal segments. Because of such discontinuous crystal distribution, the strength of TC-L in the position between adjacent crystal segments is even lower than the average strength of control sample, because there was mostly amorphous organization rather than crystals in these regions [Figure 8(b)]. Thus, during the tensile testing, the rupture preferred to take place in these positions because of the stress concentrate, which led to the decrease of the maximum strength. The fracture of TC-L always occurred in these junctions, and the corresponding fracture surface was smooth and featureless. So, the higher strength of TC-H could be ascribed into its consecutive crystal structures and the transverse linking between adjacent lamellae, compared to TC-L.

All the above results were obtained from the thin film, but the corresponding conclusion could be validly extrapolated into the bulk sample. In particular, the results provided fruitful information for the development of homogeneous fiber reinforced PLLA composite. The PLLA/PDLA blend fiber annealed below the melting point of α crystal (e.g., 145°C) can be directly used for the melt process of PLLA, for the presence of SC improves the heat resistance of blend fiber. Meanwhile, the α crystal in the fiber can enhance the interfacial interaction between fiber and matrix via epitaxial crystallization, and the generation of TC with high nucleation density benefits the integral strength of the composite.

CONCLUSIONS

The present work reported the fracture behaviors and mechanical properties of PLLA TCs with different morphologies. For TC-H, the lamellae were close to each other because of the high nucleation density. The effective linking was formed between the adjacent lamella during crystallization, which led to a high transverse strength, as well as the intense plastic deformation during fracture process. For TC-L, between the adjacent crystal segments, it was the amorphous region rather than crystal skeleton. Thus the final rupture of TC-L preferred to take place in the boundary of crystal segments. As a result, the mechanical properties of TCs, as well as the overall strength of sample were dependent on the morphologies of TCs. Although the width proportion of TC-H merely accounts for 4.5%, the strength was increased by 8.1% after removing the initial fiber. This value could reach to 12.6% while the fiber was preserved in the sample, because of the presence of homogeneous epitaxial crystallization between the fiber containing α-form crystal and PLLA matrix. On the contrary, the TC-L exhibited a negative impact on the mechanical property, because of its discontinuous crystal distribution. The present investigation may provide new insight into the preparation and development of self-reinforced composites of PLLA.

ACKNOWLEDGMENTS

Dujin Wang acknowledges the China National Funds for Distinguished Young Scientists (Grant No. 50925313). Xiuqin Zhang acknowledges Beijing Nova Program (2011016) and Beijing Municipal Natural Science Foundation (KZ201310012014).

REFERENCES

1. Quan, H.; Li, Z. M.; Yang, M. B.; Huang, R. *Compos. Sci. Technol.* **2005**, *65*, 999.

2. Urayama, H.; Kanamori, T.; Fukushima, K.; Kimura, Y. *Polymer* **2003**, *44*, 5635.

3. Nagae, S.; Otsuka, Y.; Nishida, M.; Shimizu, T.; Takeda, T.; Yumitori, S. *J. Mater. Sci. Lett.* **1995**, *14*, 1234.
4. Felix, J. M.; Gatenholm, P. *J. Mater. Sci.* **1994**, *29*, 3043.
5. Zhang, M. Q.; Xu, J. R.; Zhang, Z. Y.; Zeng, H. M.; Xiong, X. D. *Polymer* **1996**, *37*, 5151.
6. Amash, A.; Zugenmaier, P. *Polymer* **2000**, *41*, 1589.
7. Wu, C. M.; Chen, M.; Karger-Kocsis, J. *Polymer* **2001**, *42*, 129.
8. Saujanya, C.; Radhakrishnan, S. *Polymer* **2001**, *42*, 4537.
9. Chen, E. J. H.; Hsiao, B. S. *Polym. Eng. Sci* **1992**, *32*, 280.
10. Huson, M. G.; McGill, W. J. *J. Polym. Sci. B Polym. Phys.* **1985**, *23*, 121.
11. Moon, C. K. *J. Appl. Polym. Sci.* **1994**, *54*, 73.
12. Folkes, M. J.; Hardwick, S. T. *J. Mater. Sci. Lett.* **1987**, *6*, 656.
13. Wang, C.; Hwang, L. M. *J. Polym. Sci. B Polym. Phys.* **1996**, *34*, 1435.
14. Gati, A.; Wagner, H. D. *Macromolecules* **1997**, *30*, 3933.
15. HeppenstallButler, M.; Bannister, D. J.; Young, R. *J. Composites Part A* **1996**, *27*, 833.
16. Devaux, E.; Caze, C. *J. Adhes. Sci. Technol.* **2000**, *14*, 965.
17. Wen, T.; Xiong, Z.; Liu, G.; Zhang, X.; de Vos, S.; Wang, R.; Joziasse, C. A. P.; Wang, F.; Wang, D. *Polymer* **2013**, *54*, 1923.
18. Sun, L.; Jia, Y.; Ma, F.; Zhao, J.; Han, C. C. *Macromol. Mater. Eng.* **2008**, *293*, 194.
19. Petermann, J.; Broza, G.; Rieck, U.; Kawaguchi, A. *J. Mater. Sci.* **1987**, *22*, 1477.
20. Kestenbach, H.-J.; Loos, J.; Petermann, J. *Polym. Eng. Sci.* **1998**, *38*, 478.
21. Na, B.; Zhang, Q.; Wang, K.; Li, L.; Fu, Q. *Polymer* **2005**, *46*, 819.
22. Park, S.-D.; Todo, M.; Arakawa, K. *J. Mater. Sci.* **2004**, *39*, 1113.

SGML and CITI Use Only
DO NOT PRINT